20

Laser engineering of microbial systems: a new tool for microbiology

© N.V. Minaev[1], V.S. Zhigarkov[1], V.S. Cheptsov[1,2], V.I. Yusupov[1]

[1] Institute of Photon Technology, Kurchatov Complex Crystallography and Photonics, Research Center „Kurchatov Institute“, 108840, Troitsk, Moscow, Russia
[2] Lomonosov Moscow State University, Soil Science Faculty, 119991 Moscow, Russia

e-mail: minaevn@gmail.com

Received December 11, 2023
Revised January 09, 2024
Accepted January 16, 2024

One of the new areas of laser bioprinting is laser engineering of microbial systems (LEMS). This technology involves controlled transfer of gel microdroplets containing microorganisms from a donor substrate to acceptor media using a nanosecond laser pulse. During such transfer, living systems are affected by various physical factors: radiation, shock waves, temperature surges. The work carried out a study of the effect on *Escherichia coli* cells of nanoparticles that are formed during the destruction of a thin gold absorbent coating of the donor plate. It has been shown that the sizes of these nanoparticles, their concentration in the colloid, and the ξ-potential depend significantly on the laser pulse energy. It has been established that Au nanoparticles have a certain effect on the kinetics of microbial growth. A systematization of the main physical factors influencing microorganisms during their laser-induced spatial transfer has been carried out, and the most important scientific results from a practical point of view obtained using promising LEMS technology have been analyzed.

Keywords: laser bioprinting, laser engineering of microbial systems, LEMS, direct laser-induced transfer, microbiology, impact factors.

DOI: 10.61011/0000000000

Introduction

Microbiology and medicine are currently badly in need of a technique capable of widening the set of cultured microorganisms [1]. This is required, for example, to find new antibiotic producers [2] and biologically active substances [3]. The problem depth is in the fact that more than 99% microorganisms are not cultured by traditional methods and are a kind of „microbial dark matter“ [4].

This challenging task may be solved by an extensively developed technique of laser engineering of microbial systems (LEMS) [5], and approaches associated with single-cell laser-assisted bioprinting [6,7]. LEMS uses pulsed laser emission to transfer microscopic gel drops with microorganisms directly into a culture medium [8,9]. When isolating cells from natural environments, such approach helps maintain the natural environment of microorganisms and remove unwanted interactions between antagonistic species [10].

Live microsystems are exposed to various physical factors during laser-induced transfer: 1) direct laser irradiation, 2) shock waves, 3) pulsed heating and 4) dynamic impacts in acceleration and „landing“ [11–15].

Nanoparticles of thin metal absorbing coating on a donor substrate is another factor affecting microorganisms in laser-induced transfer [16–19]. Nanoparticles of various metals are known to have different effect on microorganisms [20–22]. Investigation of the effect of nanoparticles formed during bioprinting on the physiological state of microorganisms and, in particular, on their growth characteristics and dynamics is of special interest.

The study investigates the size distribution of nanoparticles formed from a thin absorbing gold layer exposed to a laser pulse with various energies and identifies their influence on *Escherichia coli* cells. In addition, an attempt was made to systemize the main physical factors affecting microorganisms in laser-induced spatial transfer and the most practically important research findings achieved using the LEMS technique were analyzed.

Materials and methods

The LEMS system is based on a 1064 nm 8 ns pulsed laser [9]. Using a galvanoscanning systems and F-theta-lens, laser beam is focused into spot 30 μm in diameter on $\sim$ 50 nm absorbing metal films of the donor plate. For the LEMS technique, the absorbing coating is applied to a $\sim$ 200 μm hydrogel layer (1.5−2% hyaluronic acid water solution) with the biomaterial. The laser pulse exposure results in vigorous heating of the absorbing film material with further formation of a vapor-gas bubble resulting in formation of a hydrogel jet and microdrop transfer to acceptor media.

The research was focused on *Escherichia coli* strain ATCC-25922 and nanoparticles synthesized using laser pulses identical to those used for LEMS [23]. Au nanoparticles (AuNP) produced by ablation of a 50 nm Au layer with YLPM-1-4x200-20-20 1064 nm 8 ns optical

fiber laser (JSC NTO „IRE-Polyus“, Russia) at two pulse energies — 16 and 45 μJ were used. Ablation of metal films on donor substrates was conducted in milli-Q water, water volume in the cell was equal to 3 ml, the number of pulses for each energy was 225000. Nanoparticle synthesis using the nanosecond laser system is described in detail in [23]. Dynamic light scattering (DLS) method and a Zetasizer Ultra (Malvern Panalytical) analyzer were used to measure the sizes, concentration and ξ-potential of the synthesized particles. The obtained nanoparticles and microstructures were examined using Helios Nanolab 600i scanning electron-ion microscope (FEI, United States).

For all experiments, the bacterial biomass was grown in LB broth (Merck, Germany) on a shaker at room temperature (23−25°C) during two days. Then the biomass was gathered by centrifugation during 3 min at 13400 rmp and washed three times in phosphate-buffer saline (PBS).

Then, PBS cell suspension absorbance vs cell concentration curves were drawn *E. coli*. For this, a set of two-fold dilutions of PBS cell suspensions was prepared and their absorbance was measured using iMark plan-table photometer (BioRad, USA) at 595 nm. In the same suspensions, bacterial cell count was measured by the epi-fluorescent microscopy method with acridine orange using Primo Star (Zeiss, Germany) with AmScope epifluorescent system (AmScope, USA). The curves were further used to prepare suspensions with specified cell concentrations.

To assess the effect of nanoparticles on the viable cell count, *E. coli* suspensions in PBS with concentrations $7.5 \cdot 10^5$ and $7.5 \cdot 10^3$ cell/ml were prepared. Then, 100 μl of cell suspension was mixed with 100 μl of nanoparticle suspension preliminary treated in NU20 ultrasonic bath (Nordberg, China) during 1 h, and with sterile distilled water (dH_2O) used as control. Thus, suspensions with cell concentrations *E. coli* $3.8 \cdot 10^5$ and $3.8 \cdot 10^3$ cell/ml, concentrations of nanoparticle synthesized at 16 and 45 μJ, $6 \cdot 10^{11}$ and $1.1 \cdot 10^{11}$ particles/ml, respectively, in 0.5X PBS. Suspensions were incubated with vortexing at 1000 rpm during 2 h. Then, these suspensions were used to prepare a series of ten-fold dilutions in 0.5X PBS and plated on LB solid medium in five replicates. After incubation during 24 hours at +37°C, colony count was recorded.

To assess the effect of nanoparticles on physiological state of bacteria, *E. coli* growth kinetics was studied in the presence of nanoparticles. For this, *E. coli* suspensions were prepared in 2X LB broth with concentrations $7.5 \cdot 10^5$ cell/ml. Then, 100 νl of the cell suspension and 100 μl of sonic nanoparticle or dH_2O were placed into wells of a 96-well plate. Thus, the plate wells contained $3.8 \cdot 10^5$ cell/ml *E. coli* in 1X LB medium and nanoparticles synthesized at 16 and 45 μJ in concentrations $6 \cdot 10^{11}$ and $1.1 \cdot 10^{11}$ particles/ml, respectively. Also, to control possible absorbance variation due to water evaporation and to control possible contamination (including cross contamination), some plate wells were filled with solutions without *E. coli* cells. Then the plate was placed in Sunrise plate photometer (Tecan, Switzerland), and absorbance was recorded at 620 nm every 30 min during 238 h (about 10 days) with vigorous plate shaking during 30 s before each measurement. Incubation was carried out at room temperature (23−25°C).

Table 1. AuNP characteristics measured by the DLS method

Energy per pulse, μJ	Mean hydrodynamic diameter , nm	Concentration pcs/ml	ξ potential mV
16	46 ± 4	$1.2 \cdot 10^{12}$	−5.4
45	82 ± 13	$2.1 \cdot 10^{11}$	−32.4
	416 ± 28	$1.5 \cdot 10^{8}$	

Kinetic curves were analyzed using Microsoft Office Excel, RStudio v. 4.1.2 (gcplyr and growthcurver) and Statistica 8.0. Before the analysis using Microsoft Office Excel, data normalization was carried out by subtraction of the least measured value from the data recorded in all measurement points. Curve smoothing (noise removal) was carried out by consecutively used moving median and moving average methods at $n = 3$ [24]. Then, parameters (lag phase duration [25], area under curve, maximum growth rate, etc.) of each kinetic curve were calculated using gcplyr [24] and growthcurver [26], then significance of differences was defined by the Mann-Whitney U test using Statistica 8.0; significance of differences in the bacterial colony count was determined in the same way. The curves were analyzed by the principal component method using Statistica 8.0.

Findings and discussion

Figure 1 shows tubes with gold nanoparticle suspension prepared in conditions used for the LEMS technique at various laser pulse energies. With energy increase, the suspension looks darker which may be indicative of an increase in sizes of the obtained nanoparticles as well as of an increase in their concentration. The typical maroon color of the formed colloidal solution is explained by plasmon absorption of AuNP (Detail in Figure 1, *a*), whose absorption wavelength is within the visible range. The DLS measurements have shown that nanoparticles with narrow size distribution (in Figure 1, *b*) 46 ± 4 nm (Table 1) are synthesized at $E = 16\,\mu$J. At $E = 45\,\mu$J, size distribution is bimodal and the mean hydrodynamic diameter of AuNP is 82 ± 13 and 416 ± 28 nm. It can be easily defined by AuNP sizes and concentration (Table 1) that 1 ml of suspension for $E = 16\,\mu$J contain 1 mg Au, and for $E = 45\,\mu$J - contain −1 mg and 0.1 mg of fine and coarse grain size, respectively.

Stability of colloidal solutions is widely known to be associated with zeta potential to a great extent. Whilst $\xi = 30$ mV (positive or negative) is treated as a typical value for nominal separation o low-charged and high-charged

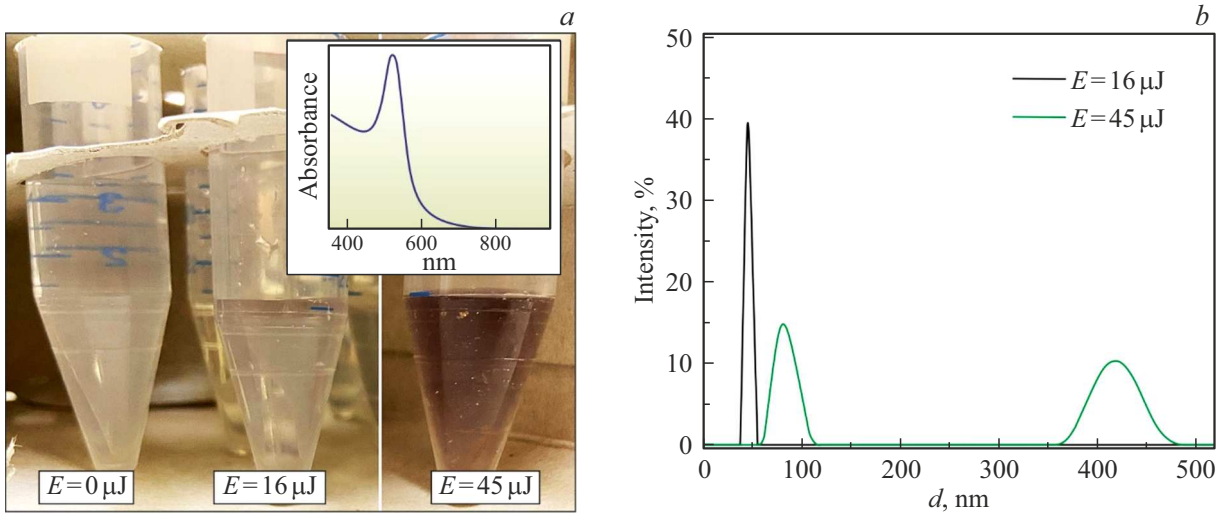

Figure 1. AuNP ablated at various laser pulse energies. (*a*) Photo of nanoparticle suspension tubes. The inset shows a typical absorption spectrum for AuNP. (*b*) AuNP size distribution using the DLS method.

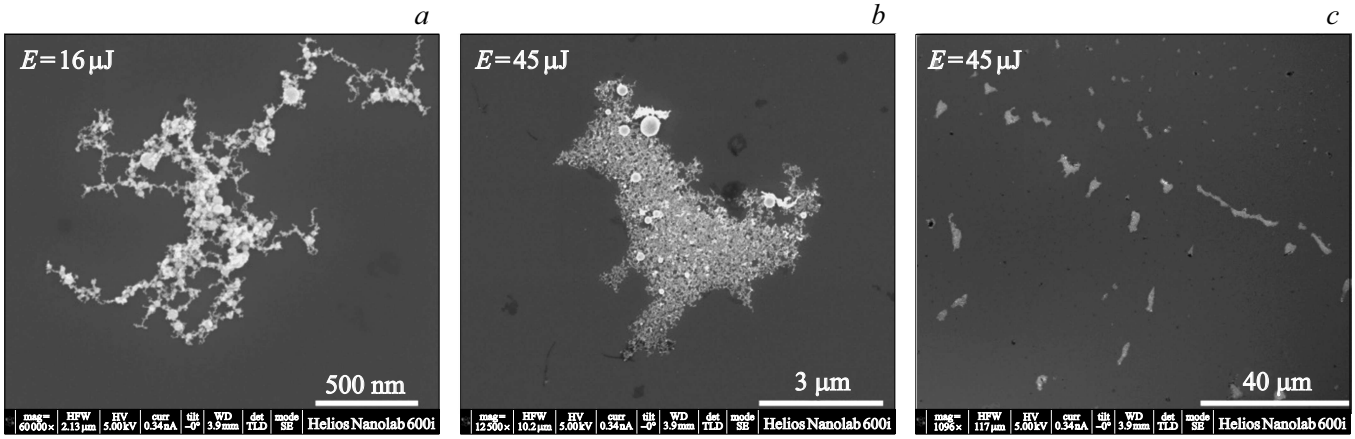

Figure 2. SEM images of AuNP on the silicon plate surface synthesized at various laser pulse energies.

surfaces. Table 1 shows that ξ potential of the suspension prepared at $E = 16\,\mu$J is equal only to -5.4 mV. This is indicative of low stability of the colloidal system which may result in AuNP coagulation and settlement. At $E = 45\,\mu$J, absolute ξ potential exceeds 30 mV which is indicative of good stability of the prepared suspension [27].

Figure 2 shows SEM images of AuNP seeded on the silicon plate surface. At $E = 16\,\mu$J, quite small nanoparticles are formed and gather in shapeless clods with partially fractal structure on the silicon plate surface. When energy of $E = 45\,\mu$J was used, relatively large submicroparticles and microparticles are seen on the SEM images in addition to fine-grain particles. We suppose that impact separation of the gold film from the glass surface takes place in addition to ablation in this case.

Incubation in the presence of nanoparticles did not influence the *E. coli* colony count. Colony count in all experiment cases was $96 - 99\%$ of the count measured by the cell suspension absorbance analysis. Thus, the exposure to nanoparticles during 2 h did not result in bacteria death.

During culturing in liquid media in the presence of nanoparticles, bacterial growth was also observed in all experiment cases, and all growth curves have a logistic curve shape (Figure 3). Curves drawn when introducing AuNP synthesized at $E = 16\,\mu$J compared with the control were characterized by the increase in mean lag phase, area under curve, population doubling time, logistic curve inflection point achievement time and medium capacity parameter, however, the differences were not statistically significant ($p > 0.05$) (Table 2). When there are no changes in the main growth characteristics, the absorbance of medium with nanoparticles during $29 - 85$ h of culturing was significantly ($p < 0.05$) higher than that of the control.

Kinetic curves in culturing with nanoparticles produced using pulses with $E = 45\,\mu$J significantly differed both from the control and other studied nanoparticles. Increase in lag phase duration, decrease in growth rate, area under curve,

Table 2. Parameters of *E. coli* growth curves (mean ± standard deviation) depending on the introduction of AuNP synthesized at various laser pulse energies. Statistically significantly different values are denoted by different letters

Exposure	Lag phase, h	Area under	k, medium capacity	r, growth rate	Logistic curve inflection point time, h	Population doubling time, h
dH_2O	1.7 ± 0.3^a	214.1 ± 4^a	0.96 ± 0.017^a	0.29 ± 0.004^a	14.8 ± 0.2^a	2.43 ± 0.03^a
Au, 16 μJ	2.5 ± 1.3^a	223.6 ± 5.4^a	1.01 ± 0.028^a	0.27 ± 0.018^a	15.2 ± 0.7^a	2.56 ± 0.17^a
Au, 45 μJ	4.8 ± 0.6^b	199.8 ± 2.4^b	0.9 ± 0.011^b	0.9 ± 0.011^b	16.4 ± 0.5^b	2.78 ± 0.01^b

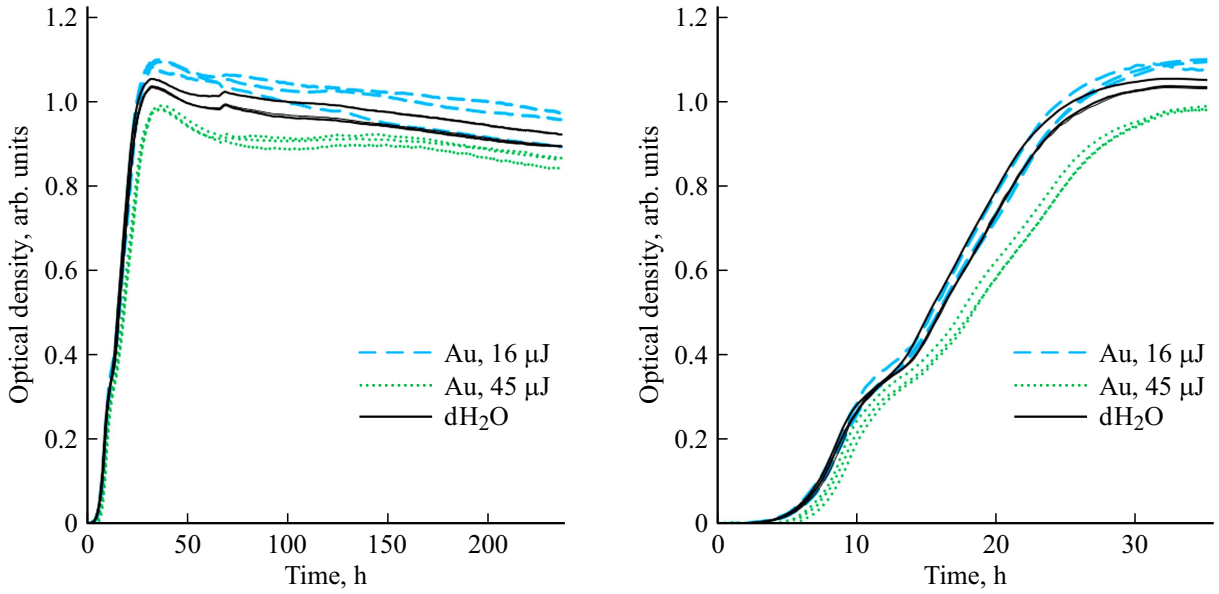

Figure 3. *E. coli* growth curves depending on the injection of AuNP synthesized at various laser pulse energies. Curves after normalization and noise removal are shown. Left — curves drawn throughout the measurement period (238 h), right — the same curves, but drawn during the first 35 h of measurements.

medium capacity and increase in population doubling time were identified.

For the principal component analysis, the curves recorded during introduction of nanoparticles synthesized at $E = 45\,\mu$ J are grouped separately from other curves (Figure 4), that is also indicative of the bacterial growth characteristics.

Thus, a slight, but valid impact of gold particles on a set of kinetic parameters of *E. coli* was found, while the highest influence was exerted by the nanoparticles synthesized at $E = 45\,\mu$J.

At this point, quite many studies have been carried out to investigate the effect of AuNP formed in laser bioprinting on live cells. Low or no any cytotoxicity of nanoparticles for mammal cells was reported [28–30]. However, the effect of such nanoparticles on microorganisms has not been studied before. Our data agree with the findings obtained for mammal cells — nanoparticles had no effect on the *E. coli* cell count and slight impact on the cell growth. Antibacterial effect of AuNP synthesized by other methods has been much better studied. It has been found that pure AuNP generally do not have a bactericidal effect,

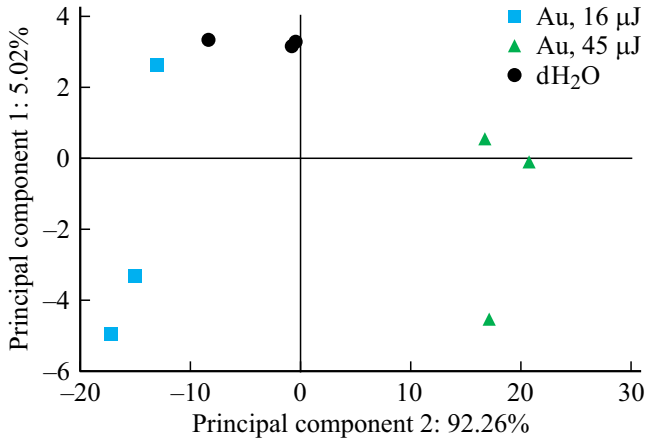

Figure 4. *E. coli* growth curves in principal component space.

however, they may show bactericidal activity in presence of other substances (for example, in formation of organic Au complexes) [31]. Whilst in some cases, cytotoxic

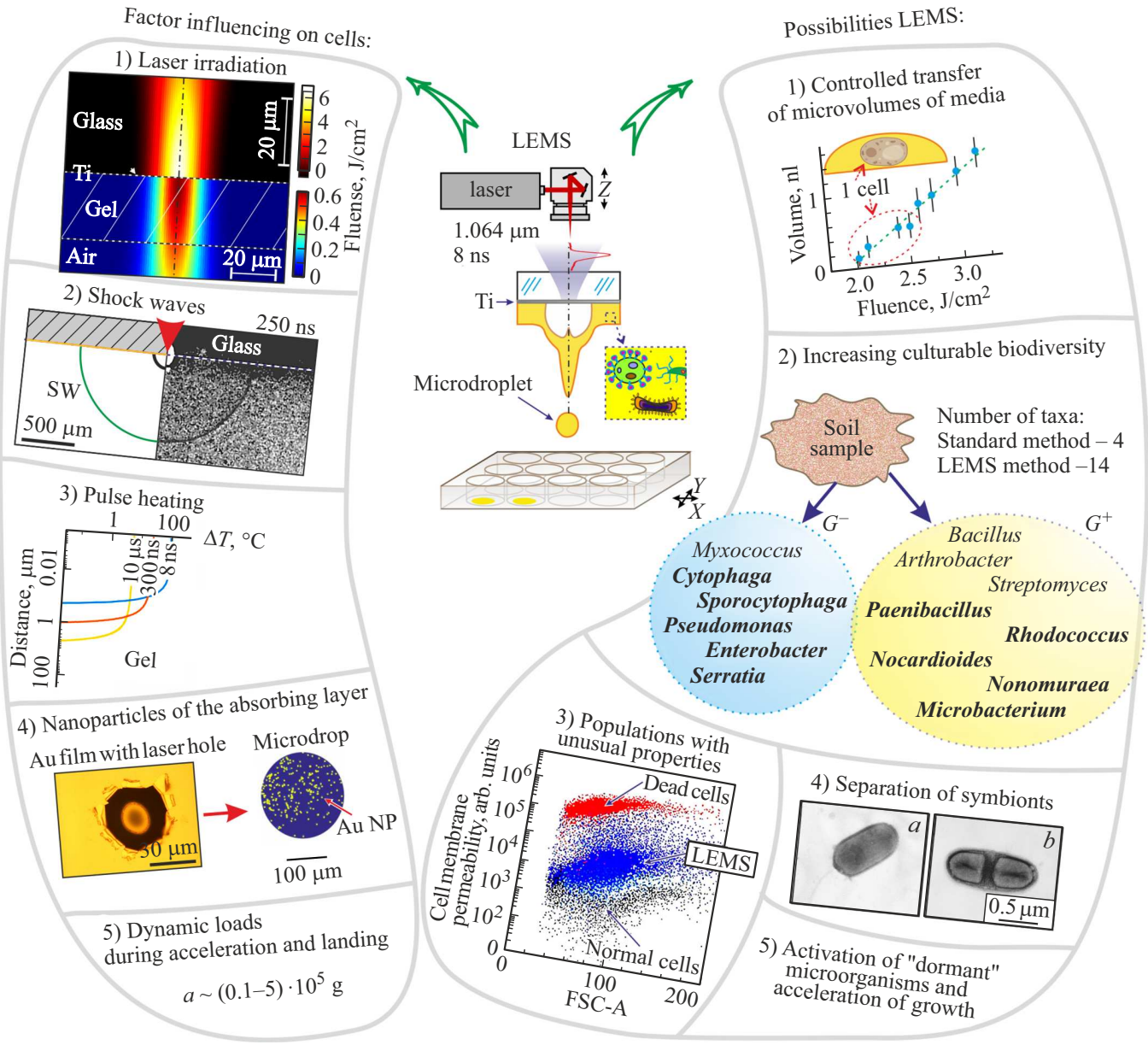

Figure 5. LEMS technique: physical factors of impact on microorganisms and the most significant opportunities.

effect of pure AuNP synthesized by other methods was reported [32,33]. It is known that the effect of nanoparticles on cell depends on many parameters — nanoparticle concentration, shape, size and composition [34–36], that explains the absence of such effects in our study.

It should be noted that we had studied a selection of nanoparticles synthesized during a lot of laser pulses and, therefore, averaged by their characteristics and concentrations. However, in case of single pulses, various number of nanoparticles may be formed that differ in several parameters (shape, size) [34,37,38]. As mentioned above, these parameters may have a considerable impact on the effects caused by nanoparticles. Therefore, it can be suggested that slightly different conditions occur at the initial stages of cell population growth during laser-induced transfer of each gel microdrop with microorganisms. The obtained data partially explain the previously observed effect of increasing cultivated bacterial variety when bacteria are isolated from soils using LEMS compared with microbiological inoculation [39,40]. Laser-assisted bioprinting from complex natural media probably not only ensures spatial separation of microbial cells, but also increases the number of physiological states and/or initial conditions of microorganism cultivation.

Another goal of our study was to systemize the main physical factors that affect microorganisms in laser bioprinting and the most practically important research findings obtained at this point using the LEMS technique to be

developed. Figure 5 shows a schematic diagram of physical factors that affect the microorganism cells during transfer and the most considerable capabilities of LEMS in terms of microbiology.

Using various investigations, the optimum parameters were defined to ensure stable transfer of microdrops with the specified size [41]. It has been found that live systems in the gel are exposed to direct laser irradiation with $F = 0.6\,\mathrm{J/cm^2}$ (factor 1 in Figure 5) at the optimum surface densities of laser pulse ($F_0 = 1 - 4\,\mathrm{J/cm^2}$). Shadow imaging methods were used to record shock waves whose pressure amplitude near the absorbing coating in the gel achieves 30 MPa [42].

As for pulsed heating that is critical for live systems (Factor 3), then it has been found that the maximum temperatures of the absorbing coating achieved almost 3000°C for Au and exceed 3000°C for Ti. It is strange that only a very thin $\sim 1\,\mu$m layer is heated up to ~ 100°C in this case in the hydrogel adjacent to the coating during the laser pulse time [43]. In other words, it is fair to say that temperature damage may occur only in microorganisms that are in the laser spot area and immediately adjacent to the absorbing coating.

Considerable heating of the metal film results in film failure with formation of holes [40] and occurrence of nanoparticles in the hydrogel. However, almost all nanoparticles remain on the donor substrate and only 0.5 to 2.5% is transferred with a microdrop to the acceptor surface [39,44] (Factor 4 in Figure 5). Whilst the nanoparticles transferred with live systems may affect the lag phase duration and microorganism growth rate. Using the high-speed video recording, it was found that the gel microjet velocity was $20 - 50$ m/s, and dynamic loads (Factor 5) are within $100 - 5000\,\mathrm{km/s^2}$ [5,39], which ensures the transfer of live objects without considerable damage [12,14,15,44].

The microbiological investigations have shown the LEMS performance that, as we believe, is associated with the capability of controlled and delicate transfer of microvolumes from 0.1 nl, when only one cell is contained in each microdrop at the initial concentration $(0.2 - 1) \cdot 10^6$ cell/ml. It has been reliably determined that LEMS facilitates considerable increase in the cultivated biodiversity [5] and allows isolating bacteria that are difficult to be cultured or cannot be cultured by standard methods (2 on the right-hand side in Figure 1). The technique results in the occurrence of populations with unusual properties (3 on the right-hand side in Figure 1). Thus, the permeability of cell membranes increases after the transfer [43]. LEMS facilitates successful isolation of pure cultures [8] and separation of stable symbionts [13] (4 on the right-hand side in Figure 1). Thus, it was the first time when a stable binary culture obtained from hot springs in Chukotka was separated. The isolated strain was assigned to a new class called *Tepidiforma bonchosmolovskayae* [45].

Conclusion

The study investigated the characteristics of AuNP formed as a result of failure of the thin gold coating on the donor plate during laser bioprinting. It is shown that sizes, concentration in colloid and ξ potential of these nanoparticles depend considerably on the laser pulse energy. It is shown by the example of *Escherichia coli* cells that such nanoparticles may have particular impact on the microorganism growth kinetics. Systematization of the main physical factors affecting microorganisms in laser-induced spatial transfer was carried out and the most practically important research findings achieved using the LEMS technique were analyzed. The knowledge accumulated in this field suggest that the new technique that is being developed is a new interesting microbiological tool and has a significant potential for practical applications in biotechnology and medicine.

Funding

The study was supported by the Russian Science Foundation (№ 20-14-00286) in terms of LEMS knowledge systematization and microbiological research, and also partially supported by the state order of Research Center „Kurchatov Institute“ in terms of laser synthesis of materials to study AuNP impact on microorganisms and the use of resource center equipment of Research Center „Kurchatov Institute“.

Conflict of interest

The authors declare that they have no conflict of interest.

References

[1] W.H. Lewis, G. Tahon, P. Geesink, D.Z. Sousa, T.J.G. Ettema. Nat. Rev. Microbiol., **19** (4), 225 (2021). DOI: 10.1038/s41579-020-00458-8
[2] J. Clardy, M.A. Fischbach, C.T. Walsh. Nat. Biotechnol., **24** (12), 1541 (2006). DOI: 10.1038/nbt1266
[3] J.V. Pham, M.A. Yilma, A. Feliz, M.T. Majid, N. Maffetone, J.R. Walker, E. Kim, H.J. Cho, J.M. Reynolds, M.C. Song, et al. Front. Microbiol., **19** (4), 10 (2019). DOI: 10.3389/fmicb.2019.01404
[4] A. Dance. Nature, **582**, 301 (2020). DOI: 10.1038/d41586-020-01684-z
[5] V.I. Yusupov, M.V. Gorlenko, V.S. Cheptsov, N.V. Minaev, E.S. Churbanova, V.S. Zhigarkov, E.A. Chutko, S.A. Evlashin, B.N. Chichkov, V.N. Bagratashvili. Laser Phys. Lett., **15** (6), 065604 (2018). DOI: 10.1088/1612-202X/aab5ef
[6] P. Liang, B. Liu, Y. Wang, K. Liu, Y. Zhao, W.E. Huang, B. Li. Appl. Environ. Microbiol., **88** (3), e01165-21 (2022). DOI: 10.1128/aem.01165-21
[7] Y. Deng, P. Renaud, Z. Guo, Z. Huang, Y. Chen. J. Biol. Eng., **11** (1), 2 (2017). DOI: 10.1186/s13036-016-0045-0
[8] V.S. Cheptsov, S.I. Tsypina, N.V. Minaev, V.I. Yusupov, B. Chichkov. Int. J. Bioprinting, —bf 5 (1), 1 (2018). DOI: 10.18063/ijb.v5i1.165

[9] N.V. Minaev, V.I. Yusupov, B.N. Chichkov. Patent RF, RU198221U1 (2020). (in Russian)
[10] J. Feichtmayer, L. Deng, C. Griebler. Front. Microbiol., **8** (2017). DOI: 10.3389/fmicb.2017.02192
[11] N.R. Schiele, D.T. Corr, Y. Huang, N.A. Raof, Y. Xie, D.B. Chrisey. Biofabrication, **2** (3), 032001 (2010). DOI: 10.1088/1758-5082/2/3/032001
[12] H.Q. Xu, J.C. Liu, Z.Y. Zhang, C.X. Xu. Mil. Med. Res., **9** (1), 1 (2022). DOI: 10.1186/s40779-022-00429-5
[13] Ž.P. Kačarević, P.M. Rider, S. Alkildani, S. Retnasingh, R. Smeets, O. Jung, Z. Ivanišević, M. Barbeck. Materials (Basel), **11** (11),(2018). DOI: 10.3390/ma11112199
[14] J. Adhikari, A. Roy, A. Das, M. Ghosh, S. Thomas, A. Sinha, J. Kim, P. Saha. Macromol. Biosci., **21** (1), (2021). DOI: 10.1002/mabi.202000179
[15] B. Hopp, T. Smausz, N. Barna, C. Vass, Z. Antal, L. Kredics, D. Chrisey. J. Phys. D. Appl. Phys., **38** (6), 833 (2005). DOI: 10.1088/0022-3727/38/6/007
[16] H. Assad, A. Assad, A. Kumar. Pharmaceutics, **15** (1), 255 (2023). DOI: 10.3390/pharmaceutics15010255
[17] Y.N. Slavin, H. Bach. Nanomaterials, **12** (24), 4470 (2022). DOI: 10.3390/nano12244470
[18] R. Gaebel, N. Ma, J. Liu, J. Guan, L. Koch, C. Klopsch, M. Gruene, A. Toelk, W. Wang, P. Mark, et al. Biomaterials, **32** (35), 9218 (2011). DOI: 10.1016/j.biomaterials.2011.08.071
[19] E. Pagés, M. Rémy, V. Kériquel, M.M. Correa, B. Guillotin, F. Guillemot. J. Nanotechnol. Eng. Med., **6** (2), 021005 (2015). DOI: 10.1115/1.4031217
[20] J.H. Niazi, M.B. Gu. *Toxicity of Metallic Nanoparticles in Microorganisms- a Review. In Atmospheric and Biological Environmental Monitoring* (Springer Netherlands, Dordrecht, 2009), pp. 193–206. DOI: 10.1007/978-1-4020-9674-7_12
[21] I.A. Mamonova, I.V. Babushkina, I.A. Norkin, E.V. Gladkova, M.D. Matasov, D.M. Puchin'yan. Nanotechnologies Russ., **10** (1–2), 128 (2015). DOI: 10.1134/S1995078015010139
[22] M.R. Khan, K.M. Fromm, T.F. Rizvi, B. Giese, F. Ahamad, R.J. Turner, M. Füeg, E. Marsili. Part. Part. Syst. Charact., **37** (5), 1 (2020). DOI: 10.1002/ppsc.201900419
[23] V.S. Zhigarkov, E.V. Ivanovskaya, K.O. Aiyyzy, A.V. Ovcharov. JTPhLet, **49** (22), 31 (2023). DOI: 10.61011/PJTF.2023.22.56597.19649
[24] M. Blazanin. Gcplyr: An R Package for Microbial Growth Curve Data Analysis. bioRxiv 2023.04.30.538883, (2023). DOI: 10.1101/2023.04.30.53888
[25] M. Peleg, M.G. Corradini. Crit. Rev. Food Sci. Nutr., **51** (10), 917 (2011). DOI: 10.1080/10408398.2011.570463
[26] K. Sprouffske, A. Wagner. BMC Bioinformatics, **17** (1), 17 (2016). DOI: 10.1186/s12859-016-1016-7
[27] A. Agha, W. Waheed, I. Stiharu, V. Nerguizian, G. Destgeer, E. Abu-Nada, A. Alazzam. *A Review on Microfluidic-Assisted Nanoparticle Synthesis, and Their Applications Using Multiscale Simulation Methods* (Springer US, 2023), vol. 18. DOI: 10.1186/s11671-023-03792-x
[28] L. Koch, O. Brandt, A. Deiwick, B. Chichkov. Int. J. Bioprinting, **3** (1), 1 (2017). DOI: 10.18063/IJB.2017.01.001
[29] L. Koch, A. Deiwick, B. Chichkov. 3D Printing and Biofabrication, **303** (2018).
[30] S. Catros, J.-C. Fricain, B. Guillotin, B. Pippenger, R. Bareille, M. Remy, E. Lebraud, B. Desbat, J. Amédé, F. Guillemot. Biofabrication, **3** (2), 025001 (2011). DOI: 10.1088/1758-5082/3/2/025001
[31] Y. Zhang, T.P. Shareena Dasari, H. Deng, H. Yu. J. Environ. Sci. Heal. Part C: Environ. Carcinog. Ecotoxicol. Rev., **33** (3), 286 (2015). DOI: 10.1080/10590501.2015.1055161
[32] K. Chandran, S. Song, S. Il Yun. Arab. J. Chem., **12** (8), 1994 (2019). DOI: 10.1016/j.arabjc.2014.11.041
[33] D. Pissuwan, C.H. Cortie, S.M. Valenzuela, M.B. Cortie. Trends Biotechnol., **28** (4), 207 (2010). DOI: 10.1016/j.tibtech.2009.12.004
[34] Y. Roiter, M. Ornatska, A.R. Rammohan, J. Balakrishnan, D.R. Heine, S. Minko. Nano Lett., **8** (3), 941 (2008). DOI: 10.1021/nl080080l
[35] A. Simon-Deckers, S. Loo, M. Mayne-L'Hermite, N. Herlin-Boime, N. Menguy, C. Reynaud, B. Gouget, M. Carriere. Environ. Sci. Technol., **43** (21), 8423 (2009). DOI: 10.1021/es9016975
[36] Y.N. Slavin, J. Asnis, U.O. Hf̈eli, H. Bach. J. Nanobiotechnology, **15** (1), 1 (2017). DOI: 10.1186/s12951-017-0308-z
[37] O.A. Lazar, A.S. Nikolov, C.C. Moise, S. Rosoiu, M. Prodana, M. Enachescu. Appl. Surf. Sci., **609**, 155289 (2023). DOI: 10.1016/j.apsusc.2022.155289
[38] S. Dittrich, S. Barcikowski, B. Gökce. Opto-Electronic Adv. **4** (1), 200072 (2021). DOI: 10.29026/oea.2021.200072
[39] M.V. Gorlenko, E.A. Chutko, E.S. Churbanova, N.V. Minaev, K.I. Kachesov, L.V. Lysak, S.A. Evlashin, V.S. Cheptsov, A.O. Rybaltovskiy, V.I. Yusupov, et al. J. Biol. Eng., **12** (1), 27 (2018). DOI: 10.1186/s13036-018-0117-4
[40] V.S. Cheptsov, E.S. Churbanova, V.I. Yusupov, M.V. Gorlenko, L.V. Lysak, N.V. Minaev, V.N. Bagratashvili, B.N. Chichkov. Lett. Appl. Microbiol., **67** (6), 544 (2018). DOI: 10.1111/lam.13074
[41] V. Yusupov, S. Churbanov, E. Churbanova, K. Bardakova, A. Antoshin, S. Evlashin, P. Timashev, N. Minaev. Int. J. Bioprinting **6** (3), 1 (2020). DOI: 10.18063/ijb.v6i3.271
[42] E. Mareev, N. Minaev, V. Zhigarkov, V. Yusupov. Photonics, **8** (9), 374 (2021). DOI: 10.3390/photonics8090374
[43] E.V. Grosfeld, V.S. Zhigarkov, A.I. Alexandrov, N.V. Minaev, V.I. Yusupov. Int. J. Mol. Sci., **23** (17),(2022). DOI: 10.3390/ijms23179823
[44] V. Zhigarkov, I. Volchkov, V. Yusupov, B. Chichkov. Nanomaterials, **11** (10), 2584 (2021). DOI: 10.3390/nano11102584
[45] T.V. Kochetkova, K.S. Zayulina, V.S. Zhigarkov, N.V. Minaev, B.N. Chichkov, A.A. Novikov, S.V. Toshchakov, A.G. Elcheninov, I.V. Kublanov. Int. J. Syst. Evol. Microbiol., **70** (2), 1192 (2020). DOI: 10.1099/ijsem.0.003902

Translated by E.Ilinskaya